High-Resolution Frequency-Domain Reflectometry by Estimation of Modulated Superimposed Complex Sinusoids

Hugo Van hamme, *Student Member, IEEE*

Abstract—**By assuming a parametric model for a linear one-port or two-port, the time-domain resolution of a vector network analyzer can be significantly improved with respect to the Rayleigh limit. The measurement problem is formulated as a nonlinear least squares parameter estimation problem involving the extremization of a cost function. An extremization algorithm with good global convergence properties is presented for the case of discontinuities of small reflectivity modeled as simple lumped *Frequency-Dependent* elements. The reflection coefficient at either port of the DUT is modeled as a superposition of *Modulated* complex sinusoids. Through optimization of a sequence of cost functions, the algorithm produces a sequence of fits for models that incorporate an increasing number of discontinuities.**

I. Introduction

CONSIDER a one-port or two-port device under test (DUT) that is a cascade of transmission lines and lumped junctions or discontinuities. An incident wave at a port of the DUT will scatter on these junctions, and the reflected wave will provide information about the type, size, and position of the discontinuities. Vector network analyzers (VNA) apply a sinusoidal incident wave and measure the reflection coefficient and possibly the insertion loss at different frequencies. The **conventional Fourier technique** transforms this measured frequency response to the time domain with an inverse discrete Fourier transform to yield an estimate of the corresponding impulse response of the DUT. Discontinuities are revealed as peaks in the reflectogram thus obtained.

The resolution (minimum separation δl of discontinuities to be distinguishable) of the conventional Fourier technique with equispaced measurement frequencies is given by the Rayleigh limit [1]:

$$\delta l \approx \frac{c_o}{2f_{\text{span}}} \tag{1.1}$$

where δl is the resolution limit in electrical length units, c_o is the velocity of light in a vacuum, and f_{span} is the difference between the highest and the lowest measurement frequency. Electrical length equals physical length divided by the relative (w.r.t. c_o) propagation velocity in the medium. The resolution obtained from analysis of frequency-domain data can be improved by introducing a frequency-domain model for both the lumped junctions and the connecting transmission lines. The increased performance is paid for with prior knowledge required to model the DUT. In previous attempts [2]–[4], the model assumptions included small, **frequency-independent** reflection coefficients for the lumped elements and (nearly) lossless transmission lines. The reflection coefficient at either port of the DUT is then modeled as a superposition of complex sinusoids or **cisoids** as a function of frequency. The estimation of the parameters in such a model is intensively studied in the literature and yields **superresolution** techniques. Among the many available methods, MUSIC [5], [6], ESPRIT [9], and nonlinear least squares estimation (NLSE) [5], [6] were applied to the reflectometry problem in [2], [3], and [4], respectively.

In this paper, the nonlinear least squares approach will be chosen. It uses a signal model that accommodates **frequency-dependent** models for the junctions. To the author's knowledge, this is the first paper that treats frequency-dependent reflections in a superresolution context. In the **first phase** (Sections III and IV), the NLSE-superresolution technique based on the simplified signal model of Section II is used. The advantages of NLSE are low threshold (see [4]) and the ability to use a parsimonious parametrization. The assumptions made in phase one include "small" discontinuities with nearly perfect connecting transmission lines at all measurement frequencies. The solution obtained using these assumptions is used as a **good** initial guess for use in a **second phase** (Section V) that tunes the parameters of a more rigorous model. This requires prior knowledge regarding the structure of the device, such that a parametric model can be compiled.

II. A Simplified Signal Model

Consider the one-port sketched in Fig. 1. Full exploitation of two-port data is postponed till the second phase. The DUT is composed of M junctions $J_k (k = 1 \cdots M)$ with frequency-dependent scattering matrix $S^{(J_k)}(f)$ and M connecting transmission lines $T_i (k = 1 \cdots M)$ of electrical length l_i, complex frequency-dependent constant of

Manuscript received May 14, 1992; revised August 10, 1992. This work was supported by the Belgian National Fund for Scientific Research (NFWO).

The author is with Vrije Universiteit Brussel, Dept. ELEC, Pleinlaan 2, 1050 Brussels, BELGIUM.

IEEE Log Number 9204339.

0018-9456/92$3.00 © 1992 IEEE

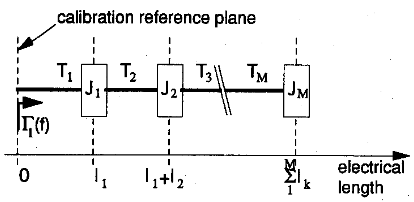

Fig. 1. DUT structure.

propagation $\gamma(f) = \alpha(f) + j\beta(f)$ and characteristic impedance $Z_{c,k}$. In this paper, the attention is restricted to lumped junctions that are of the type:

type R (real): a series resistor, a shunt conductance, a step in the characteristic impedance or a cascade of these,

type I (imaginary): a series inductor, a shunt capacitor or a cascade of these,

type C (complex): a cascade of junctions of types R and I.

Other junction models can be handled, as long as they allow an approximate cisoidal model (2.1) with known modulation function and linear amplitude parameters. The Mth junction represents the termination of the imperfect line (possibly the second VNA measurement port) and must offer a good match as well. It was shown in [4] that the reflection coefficient measured at the VNA port can be approximated as:

$$\Gamma_1(f) \approx \sum_{k=1}^{M} \left((S_{11}^{(J_k)}(f) \prod_{n=1}^{k-1} S_{12}^{(J_n)}(f) S_{21}^{(J_n)}(f) \right) \cdot \exp\left(-2(\alpha(f) + j\beta(f)) \sum_{n=1}^{k} l_n \right) \tag{2.1a}$$

provided that the magnitudes of both $S_{11}^{(J_k)}$ and $S_{22}^{(J_k)}$ are small for all k. The approximation involves neglecting the **multiple** reflections on the junctions. Assume that the total line attenuation $\alpha(f)\Sigma_1^M l_n$ is small, that $Z_{c,k}$ is nearly real, that $\beta(f)$ is essentially a linear function of frequency (small propagation dispersion), and that the nth junction can be modeled as a series impedance $Z_n(f) = z_n(f)Z_{c,n}$, a shunt admittance $Y_n(f) = z_n(f)/Z_{c,n}$ or a step in characteristic impedance $z_n = 2(Z_{c,n+1} - Z_{c,n})/(Z_{c,n+1} + Z_{c,n})$, all with $|z_n(f)| << 1$ at all measurement frequencies. The **measured** reflection coefficient can then be written as a superposition of modulated cisoids [10]:

$$\Gamma_m(f) = \sum_{k=1}^{M} C_k m_k(f) \exp\left(-j \frac{4\pi}{c_o} f \sum_{n=1}^{k} l_n \right) + w(f) \tag{2.1b}$$

where C_k is a **real-valued** amplitude parameter, and $m_k(f)$ is a complex-valued **modulation** function depending on the junction type. For type R junctions, i.e., if $z_k(f)$ is real-valued and frequency-independent, $m_k(f) = 1$; for type I junctions, i.e., $z_k(f)$ is purely imaginary and proportional to f, $m_k(f) = jf$. Extension to junctions of type C is achieved by modifying the modulated amplitude $C_k m_k(f)$ for a single index k in (2.1b) to $R_k + jfI_k$ where R_k and I_k are two amplitude parameters. The contribution $w(f)$ in (2.1b) contains the measurement noise, the calibration error, the multiple reflections and other approximation errors.

The VNA measures $\Gamma_1(f)$ at frequencies $(n_o + n)\,\Delta$ Hz with $n = 0 \cdots N - 1$ and $n_o << N$. Introduce the measurement vector $x^t = [\Gamma_m(n_o\Delta), \cdots, \Gamma_m((n_o + N - 1)\Delta)]$, (superscript "t" stands for vector and matrix transposition), the noise vector $w^t = [w(n_o\Delta), \cdots, w((n_o + N - 1)\Delta)]$, the normalized cisoidal frequencies

$$u_k = \frac{2\Delta}{c_o} \sum_{n=1}^{k} l_n \qquad (k = 1 \cdots M), \tag{2.2a}$$

the linear modulation vector $\boldsymbol{n}$, the unmodulated steering vector $\boldsymbol{e}(u)$, the linearly modulated steering vector $\boldsymbol{r}(u)$, and the quadratically modulated steering vector $\boldsymbol{q}(u)$:

$$\boldsymbol{n} = \begin{bmatrix} jn_o \\ j(n_o + 1) \\ \vdots \\ j(n_o + N - 1) \end{bmatrix},$$

$$\boldsymbol{e}(u) = \begin{bmatrix} \exp(-j2\pi u n_o) \\ \exp(-j2\pi u(n_o + 1)) \\ \vdots \\ \exp(-j2\pi u(n_o + N - 1)) \end{bmatrix} \tag{2.2b}$$

$\boldsymbol{r}(u) = \boldsymbol{n} \odot \boldsymbol{e}(u)$ and $\boldsymbol{q}(u) = \boldsymbol{n} \odot \boldsymbol{r}(u)$ where $\odot$ denotes elementwise matrix product (Hadamard product). Furthermore, let

$\boldsymbol{E}_k(u) = \boldsymbol{e}(u)$ and $\boldsymbol{a}_k \in \mathbb{R}$ if J_k is of type R;

$\boldsymbol{E}_k(u) = \boldsymbol{r}(u)$ and $\boldsymbol{a}_k \in \mathbb{R}$ if scalar if J_k is of type I;

and

$\boldsymbol{E}_k(u) = [\boldsymbol{e}(u)\boldsymbol{r}(u)]$ and $\boldsymbol{a}_k \in \mathbb{R}^2$ if J_k is of type C.

Then the simplified signal model is obtained:

$$\boldsymbol{x} = \boldsymbol{E}(\boldsymbol{u})\boldsymbol{a} + \boldsymbol{w} \tag{2.3}$$

with

$$\boldsymbol{a} = [\boldsymbol{a}_1^t, \cdots, \boldsymbol{a}_M^t]^t \in \mathbb{R}^{Q_M} \text{ with } M \leq Q_M \leq 2M$$

$$\boldsymbol{u} = [u_1, \cdots, u_M]^t \in \mathbb{R}^M$$

and

$$\boldsymbol{E}(\boldsymbol{u}) = [\boldsymbol{E}_1(u_1), \cdots, \boldsymbol{E}_M(u_M)] \in \mathbb{C}^{N \times Q_M}.$$

III. Nonlinear Least Squares Estimation (NLSE)

Consider the general NLSE problem of fitting a cisoidal model with K junctions of known type to $\boldsymbol{x}$, where K is a predefined integer number. The NLSE method minimizes $\|\boldsymbol{x} - \boldsymbol{E}(\boldsymbol{v})\boldsymbol{b}\|_2$ over the independent variables. These are the K-vector v of cisoid frequencies and the vector $\boldsymbol{b}$ of amplitudes. For notational convenience, the matrix $\boldsymbol{E}(\boldsymbol{v})$ defined in (2.3) contains as many submatrices $\boldsymbol{E}_k$ as there are entries in $\boldsymbol{v}$ (in this case K instead of M), i.e., $\boldsymbol{E}(\boldsymbol{v}) = [\boldsymbol{E}_1(v_1), \cdots, \boldsymbol{E}_K(v_K)]$. The number of columns in each of the $\boldsymbol{E}_k(v_k)$ is known to be 1 or 2 from the assumed junction type, and the total number of columns in $\boldsymbol{E}(\boldsymbol{v})$ is called Q_K. Minimization of $\|\boldsymbol{x} - \boldsymbol{E}(\boldsymbol{v})\boldsymbol{b}\|_2$ over $\boldsymbol{b}$ is a **linear** least squares problem that can be solved explicitly for each $\boldsymbol{v}$. Substitution of this solution in $\|\boldsymbol{x} - \boldsymbol{E}(\boldsymbol{v})\boldsymbol{b}\|_2$ leaves the following cost to be **maximized** (proof is formally the same as in [4]):

$$L_{x,K}(\boldsymbol{v}) = (\boldsymbol{x}^H\boldsymbol{E}(\boldsymbol{v}))_R(\boldsymbol{E}^H(\boldsymbol{v})\boldsymbol{E}(\boldsymbol{v}))_R^{-1}(\boldsymbol{E}^H(\boldsymbol{v})\boldsymbol{x})_R \quad (3.1)$$

where subscript "R" indicates the real part of a complex quantity, and superscript "H" means Hermitian transposition. The cost is indexed with $\mathbf{x}$ to stress its dependence on the measurements and with K to indicate the number of junctions or modulated cisoids present in the model. $L_{x,K}(\boldsymbol{v})$ is a nonquadratic function of the parameters $\boldsymbol{v}$ that exhibits numerous local maxima. The global maximum can be found by a **global search**, that is, maximizing by exhaustive search over a grid. The computational load of this method increases exponentially with K. Therefore, the K-dimensional global search will be replaced by a series of one-dimensional global searches that can be implemented efficiently.

For simplicity, it is assumed in the remainder of this section that all junctions are of the same type. By definition, the cisoid frequency estimates for this Kth order model are given by:

$$\boldsymbol{v}_K = \arg\max_{v_1 \cdots v_K} L_{x,K}(\boldsymbol{v}) \quad (3.2a)$$

with $\boldsymbol{v}^t = [v_1, \cdots, v_K]$. For $K = 1$, the (3.2a) is a maximization over one variable, which involves an acceptable computational load. For $K \geq 2$, the problem must be simplified. Since all junctions are of the same type, the global maximizer of $L_{x,K}(\boldsymbol{v})$ is not unique: permutation of the entries of $\boldsymbol{v}$ yields the same value of $L_{x,K}$. The algorithm outlined in the next section is based on the assumption that it is possible to find a maximizer $\boldsymbol{v}_K$, whose upper $K - 1$ entries are $\boldsymbol{v}_{K-1}$, perturbed by at most $1/(2N)$ in order of magnitude, and a new Kth component (see [10]). The underlying idea of the algorithm is to estimate the small perturbation of $\boldsymbol{v}_{K-1}$ using a linearized signal model, and this for every candidate v_K. This will require the extremization of a modified cost function over just one variable. To obtain this modified cost function, consider the Kth component of the exact solution $\boldsymbol{v}_K$.

$$v_{K,K} = \arg\max_{v_K} \{ \max_{v_1 \cdots v_{K-1}} L_{x,K}(\boldsymbol{v})\}. \quad (3.2b)$$

Written this way, the NLSE is formulated as fitting a model (3.3) to $\boldsymbol{x}$ for every choice of v_K, and then selecting the v_K that provides the best fit in the least squares sense. Hence, given v_K, a nonlinear least squares fit of the amplitudes $\boldsymbol{a}_1, \cdots, \boldsymbol{a}_K$ and frequencies $v_1 \cdots, v_{K-1}$ is sought in the model

$$\boldsymbol{x} = [\boldsymbol{E}_1(v_1), \cdots, \boldsymbol{E}_{K-1}(v_{K-1}), \boldsymbol{E}_K(v_K)] \cdot \begin{bmatrix} \boldsymbol{a}_1 \\ \vdots \\ \boldsymbol{a}_{K-1} \\ \boldsymbol{a}_K \end{bmatrix} + \boldsymbol{w}. \quad (3.3)$$

Instead of finding the optimal $[v_1, \cdots, v_{K-1}]^t$, the vector of optimal deviations $[\delta_1, \delta_2, \cdots, \delta_{K-1}]^t$ from the known vector $v_{K-1} = [v_{K-1,1}, v_{K-1,2}, \cdots, v_{K-1,K-1}]^t$ is sought. If these optimizing δ_k satisfy $|\delta_k| << 1/(2N)$, the following truncated Taylor series can be written:

$$\boldsymbol{e}(v_{K-1,k} + \delta_k) \approx \boldsymbol{e}(v_{K-1,k}) - 2\pi\delta_k\boldsymbol{r}(v_{K-1,k}) \quad (3.4a)$$

$$\boldsymbol{r}(v_{K-1,k} + \delta_k) \approx \boldsymbol{r}(v_{K-1,k}) - 2\pi\delta_k\boldsymbol{q}(v_{K-1,k}). \quad (3.4b)$$

The NLSE frequencies $v_1, \cdots, v_{K-1}$ and amplitudes $\boldsymbol{a}_1, \cdots, \boldsymbol{a}_K$ for model (3.3) can be recovered approximately from $\boldsymbol{c}$ in the linearized signal model:

$$\boldsymbol{x} = [\boldsymbol{F}(\boldsymbol{v}_{K-1}), \boldsymbol{E}_K(v_K)]\boldsymbol{c} + \boldsymbol{w} \quad (3.5)$$

with

$$\boldsymbol{c} = [\boldsymbol{c}_1^t, \cdots, \boldsymbol{c}_{K-1}^t, \boldsymbol{a}_K^t]^t$$

and

$$\boldsymbol{F}([v_1, \cdots, v_{K-1}]^t) = [\boldsymbol{F}_1(v_1), \cdots, \boldsymbol{F}_{K-1}(v_{K-1})] \in \mathbb{R}^{Nx(Q_{K-1}+K-1)}$$

where

$$\boldsymbol{F}_k(v) = [\boldsymbol{e}(v)\boldsymbol{r}(v)] \text{ and } \boldsymbol{c}_k \in \mathbb{R}^2 \text{ if } J_k \text{ is of type R,}$$

$$\boldsymbol{F}_K(v) = [\boldsymbol{r}(v)\boldsymbol{q}(v)] \text{ and } \boldsymbol{c}_k \in \mathbb{R}^2 \text{ if } J_k \text{ is of type I,}$$

$$\boldsymbol{F}_k(v) = [\boldsymbol{e}(v)\boldsymbol{r}(v)\boldsymbol{q}(v)] \text{ and } \boldsymbol{c}_k \in \mathbb{R}^3 \text{ if } J_k \text{ is of type C.}$$

For those choices of v_K where the maximizing $v_1, \cdots, v_{K-1}$ deviate more than $1/(2N)$ from the entries of $\boldsymbol{v}_{K-1}$, the linearized model (3.5) is expected to give a **poorer** fit than the correct model (3.3), since (3.5) is inadequate to describe the data. However, when v_K assumes the optimal value $v_{K,K}$ this will not be the case, since then v_K and the maximizer of the inner problem in (3.2b) are the components of $\boldsymbol{v}_K$, for which the small-δ_k assumption is valid, as demonstrated in [10]. Hence, unless the linearized model would occasionally produce a better fit for nonoptimal (in the sense of 3.2b) values of v_K, the optimal value of v_K for the linearized problem will approximate the true optimizer of (3.2b).

The estimation of $\boldsymbol{c}$ in (3.5) is a **linear** least squares problem that is easily solved and substituted in the cost as was done for $\boldsymbol{b}$. This yields a cost that is a function of v_K only, since $\boldsymbol{v}_{K-1}$ is known and fixed. Algebraic manipulations then show that the optimal v_K is the **maximizer** of:

$$s(v_K)^t T^{-1}(v_K) s(v_K) \tag{3.6}$$

with

$$s(v_K) = (E^H x)_R - (E^H F)_R (F^H F)_R^{-1} (F^H x)_R$$

and

$$T(v_K) = (E^H E)_R - (E^H F)_R (F^H F)_R^{-1} (F^H E)_R$$

where the shorthand $[F, E]$ is used for $[F(\boldsymbol{v}_{K-1}), E_K(v_K)]$. An approximate solution of the maximizer of (3.6) is found by a **one-dimensional** coarse search over v_K, the result being $\tilde{v}$. A gradient-type maximizing technique with initial guess $[\boldsymbol{v}_{K-1}^t, \tilde{v}]^t$ can then be applied to $L_{x,K}(\boldsymbol{v})$ to finally solve (3.2a) exactly. The global search grid for maximizing (3.6) has a spacing of $1/N_{FFT}$, where N_{FFT} is a power of 2 that is greater than $8N$. This resolution is sufficient, because it was shown in the appendix of [4], that for a type R junction with $n_o << N$, the width of the "humps" of $L_{x,K}$ is approximately $1/N$. The same conclusion can be drawn for type I junctions, while the double width can be found for type C junctions.

For junction type R and I, s and T are scalars; for junction type C, $s \in \mathbb{R}^2$ and $T \in \mathbb{R}^{2\times 2}$. Since $E^H E$ and $F^H F$ are independent of v_K, they must be computed only once per grid search. The entries of $(E^H x)_R$ and $(E^H F)_R$ depend on the differences between v_K and an entry $\boldsymbol{v}_{K-1}$ only and can therefore be read from a lookup table with $O(N_{FFT})$ entries. Hence, the one-dimensional global search requires little computation.

IV. Algorithm Outline—Prior Knowledge

Assume for the moment that all junctions are of the same type. The basic algorithm is:

1. Set $K = 1$. A global search and a refining gradient-type extremization are used to maximize $L_{x,1}$, the maximizer being $\boldsymbol{v}_1$ (a scalar).
2. Increment K. Maximize $L_{x,K}(\boldsymbol{v})$ by first finding the $\tilde{v}$ on the grid that maximizes the linearized-model cost (3.6) and then applying a gradient-type maximizing technique to the original cost $L_{x,K}(\boldsymbol{v})$ with initial guess $[\boldsymbol{v}_{K-1}^t, \tilde{v}]^t$. The result is called $\boldsymbol{v}_K$.
3. If $K < M$, round all entries of $\boldsymbol{v}_K$ to their closest value on the N_{FFT}-point grid and go to 2; else, the final estimate is $\boldsymbol{v}_M$.

Due to the approximations, global convergence of the algorithm is not assured. It is possible that the algorithm converges to a local maximizer of $L_{x,M}$, in particular if n_o becomes comparable to N, if the dynamic range of the signal components is large or if a multitude of junctions is separated by less than the Rayleigh limit. In the latter case, a study of the Cramér–Rao bounds reveals that an unbiased solution of the problem becomes extremely noise sensitive, i.e., even the correct solution may be of no practical use. The restriction on n_o implies that the simplified signal model must be valid at low frequencies, explaining why the attention was restricted to low-pass junctions.

The use of prior knowledge can conquer the problem of local extrema. Algorithmically, it is possible that too many components of $\boldsymbol{v}_K$ are within $1/(2N)$ of a cluster of **fewer** true frequencies of strong components that are themselves separated by less than $1/(2N)$. Escape from such a local maximum of $L_{x,K}$ is possible by removing each of the $K-1$ other cisoids from the model and adding it again by a one-dimensional search as in step 2 of the algorithm. This procedure, which is similar to alternating projection described in [7], is inserted in the algorithm after step 2. The computational load of one cycle through the algorithm is then increased to K (instead of 1) global searches.

The algorithm can handle a mixture of junction types, but the problem of local extrema becomes more acute. The **order** in which junctions of different types are added to the model becomes important. Intelligent user interaction based on prior knowledge can exclude many possibilities. Since any cisoid frequency at any intermediate stage of the algorithm is assumed to be correct within about $1/(2N)$, formula (2.2a) allows an *a posteriori* confrontation with prior knowledge regarding the DUT structure. Also, *a priori* hard bounds on the coarse search grid can be derived from structural information.

More information than just the junction type might be available; e.g., for shunt conductance or capacitor, the amplitude of the modulated cisoid is negative; for series resistor or inductor, it is positive. All points of the grid that yield an amplitude of opposite sign are excluded as potential maximizers of (3.6). For each candidate frequency v_K, the amplitude equals $T^{-1}(v_K)s(v_K)$ and can be checked without extra work.

V. Parameter Fine Tuning

Let $S(\boldsymbol{p}, f)$ be a frequency-dependent model of the scattering matrix of the passive DUT, depending on the parameters $\boldsymbol{p}$. On the other hand, the measurements $S_m(\Delta(n_o + n))(n = 0 \cdots N-1)$ of this scattering matrix are available. An NLSE approach for the two-port problem then minimizes the weighted sum $F(\boldsymbol{p})$ (over n and all measured scattering parameters) of squares of differences between the model and the measurements.

In the model $S(\boldsymbol{p}, f)$, $\boldsymbol{p}$ must contain the lengths between the junctions and other parameters characterizing the lumped junctions themselves, the **junction quantifiers** (e.g., value of a capacitor, width of a microstrip, etc.). Minimization of $F(\boldsymbol{p})$ is achieved using an iterative gradient-type technique. The cisoid frequencies can be converted to initial guesses for the electrical lengths via (2.2a). The remaining component values can easily be obtained from zero initial guesses by first minimizing $F(\boldsymbol{p})$ with the electrical lengths fixed at their initial guesses. Subsequently, $F(\boldsymbol{p})$ must be minimized over all entries of $\boldsymbol{p}$, yielding the final estimates.

VI. Experimental Results

Consider the microstrip structure shown in Fig. 2. It is built on "ordinary" epoxy/glass-fiber printed circuit board (p.c.b.) with a dielectric thickness of 1.55 mm $\pm$ 0.05 mm, a dielectric loss tangent $\tan \delta = 0.02 \pm 0.01$ and a relative dielectric constant $\epsilon_r = 4.3 \pm 0.1$. The reflection coefficient at the reference plane (in the SMA connector) is measured at 101 equispaced frequencies between 45 MHz and 2.295 GHz, i.e., $\Delta = 22.5$ MHz, $N = 101$ and $n_o = 2$. The microstrip line exhibits two steps in width and is terminated in a 47.0 $\Omega \pm 0.2$ Ω chip resistor. To make the junctions (impedance steps) frequency-dependent, two chip capacitors of 1 pF are mounted between the strip and the ground plane. The notations used for the dimensions of the DUT and the components are defined in Fig. 2. Notice that d_k is the mechanical length of transmission line T_k, while its electrical length is denoted by l_k. The SMA-to-microstrip transition consists of a 0.5-mm segment of the soldering pin of the central conductor of the connector.

The data is first processed by the conventional Fourier technique (see Fig. 3). The extrema of this bandpass impulse response do not coincide with the true positions of the junctions due to their frequency-dependent behavior and due to merging of the responses of the individual junctions. Moreover, the Rayleigh resolution is about 65 mm of one-way electrical length.

Significant reflections are expected at the connector, at both impedance-steps/capacitors and at the termination resistor. All junctions are modeled as type C junctions: for the step/capacitors this is obvious; the SMA-to-microstrip transition is of type I (see [11]), which yields a type C junction if an impedance step is present, and the resistive termination may exhibit spurious reactive elements. A model containing four type C junctions is fitted to the frequency-domain data using the algorithm outlined in Section IV:

$$\boldsymbol{x} \approx \sum_{k=1}^{4} (a_k \boldsymbol{e}(u_k) + b_k \boldsymbol{r}(u_k))$$

with u_k related to the electrical lengths by (2.2a). The electrical lengths are found to be $l_1 = 22.5$ mm, $l_2 = 88.3$ mm, $l_3 = 114.8$ mm and $l_4 = 101.5$ mm. The electrical length of 22.5 mm for the connector is obviously too large. To improve on these first results, the DUT is modeled as a cascade of perfect transmission lines and lumped elements as shown in Fig. 4.

The electrical length of an SMA connector was measured in a separate experiment and was found to be $l_1 = 12.4$ mm, and $Z_{c,1}$ was set to 50.0 Ω. These connector characteristics will be fixed in the analysis to follow and

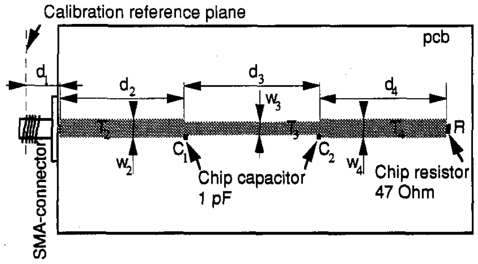

Fig. 2. Description of the DUT (drawing not to scale).

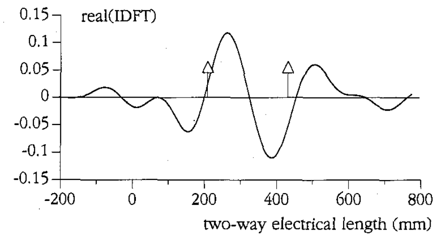

Fig. 3. The extrema of the real part of the Inverse Discrete Fourier Transform (IDFT) of the Hamming-windowed frequency-domain data do not coincide with the junction positions, making conventional Fourier techniques hard to interpret. The arrows show the position of both capacitors.

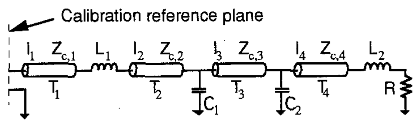

Fig. 4. Model 1 consisting of prefect transmission lines and lumped elements.

are not reestimated. With the initial values $l_2 = 98.4$ mm $(= 88.3 + 22.5 - 12.4)$, $l_3 = 114.8$ mm, $l_4 = 101.5$ mm, $L_1 = L_2 = 0$ nH, $Z_{c,2} = Z_{c,3} = Z_{c,4} = R = 50$ Ω and $C_1 = C_2 = 0$ pF, $F(\boldsymbol{p})$ as defined in Section V is minimized with l_2, l_3, and l_4 fixed, then variable. Finally, the characteristic impedance and electrical length thus obtained for each line are converted into initial estimates for the width and mechanical length of a microstrip transmission line using the microstrip design formulae of [12], and the model parameters are estimated by minimizing the least squares criterion of Section V. The model, depicted in Fig. 5, incorporates dispersion and loss in the microstrips. The resulting estimates for the lumped elements are: $L_1 = 0.30$ nH, $L_2 = 1.00$ nH, $R = 47.5$ Ω, $C_1 = 1.13$ pF and $C_2 = 1.11$ pF. The estimated microstrip dimensions are compared with measured mechanical dimensions in Table I. Since the characteristic impedance of a microstrip is basically a function of the w/t ratio (t is the dielectric thickness) and ϵ_r, the uncertainty on t and ϵ_r can explain the differences in the estimated and measured strip widths.

The quality of the fit is examined using Fig. 6. It displays the magnitude of the measured reflection coefficient and the magnitude of the residuals (the complex difference between measured and modeled reflection coeffi-

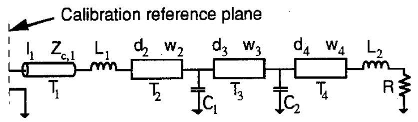

Fig. 5. Model 2 consisting of nonideal microstrip transmission lines and lumped elements.

TABLE I
THE ESTIMATED VERSUS THE MEASURED MICROSTRIP DIMENSIONS

	estimate (mm)	measured (mm)
d_2	50.8	50.5 ± 0.5
d_3	59.9	59.5 ± 0.5
d_4	51.7	51.0 ± 0.5
w_2	3.64	3.44 ± 0.05
w_3	2.93	2.87 ± 0.05
w_4	3.51	3.56 ± 0.05

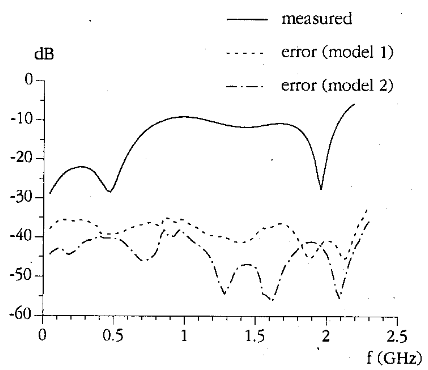

Fig. 6. Magnitude of measured reflection data (solid), magnitude of residuals for lossless-transmission-line model (dashed) and magnitude of residuals for microstrip model (dot-dash).

cient). The unmodeled behavior is more than an order of magnitude smaller than the modeled phenomena. Also, the second model performs better. The remaining modeling errors are probably mainly due to the repeatability problems caused by the flexible cables in the measurement setup and due to the poor connector and transition models.

Finally, it is worth noting that the method performed well, although the magnitude of the reflection coefficient reaches values over 0.6, a serious violation of the "small discontinuities" assumption.

VII. CONCLUSIONS

A nonlinear least squares estimation method for time-domain analysis from frequency-domain measurements of a DUT was presented. Estimation is based on a parsimonious model that requires a low reflectivity assumption. The method copes with frequency-dependent reflection. It was shown how prior knowledge can (and should) be used to improve the performance of the algorithm. Analysis of experimental data illustrated the potential of the method.

REFERENCES

[1] *Student Guide for Basic Network Measurements Using the HP8510A Network Analyzer System.* Hewlett-Packard Course HP8510A+24D, ed. 2.0, Dec. 1986.

[2] H. Yamada, M. Ohmiya, and Y. Ogawa, "Superresolution techniques for time-domain measurements with a network analyzer," *IEEE Trans. Antennas Propagat.*, vol. 39, pp. 177–183, Feb. 1991.

[3] Z. A. Marićević, T. K. Sarkar, and Y. Hua, "Time-domain measurements with the Hewlett-Packard network analyzer HP8510 using the matrix pencil method," *IEEE Trans. Microwave Theory Tech.*, vol. 39, pp. 538–547, March 1991.

[4] H. Van hamme, "High resolution frequency-domain reflectometry," *IEEE Trans. Instrum. Meas.*, vol. 39, pp. 369–375, April 1990.

[5] P. Stoica and A. Nehorai, "MUSIC, maximum likelihood, and Cramér-Rao bound," *IEEE Trans. Acoustics, Speech, Signal Processing*, vol. 37, pp. 720–741, May 1989.

[6] S. M. Kay, *Modern Spectral Estimation: Theory and Application.* Englewood Cliffs, NJ: Prentice Hall, 1988, ch. 13.

[7] I. Ziskind and M. Wax, "Maximum likelihood localization of multiple sources by alternating projection," *IEEE Trans. Acoustics, Speech, and Signal Processing*, vol. 36, pp. 1553–1560, Oct. 1988.

[8] H. Van hamme, "Maximum likelihood estimation of superimposed complex sinusoids in white Gaussian noise by reduced effort coarse search (RECS)," *IEEE Trans. Acoustics, Speech, and Signal Processing*, vol. 39, pp. 536–538, Feb. 1991.

[9] R. Roy, A. Paulraj, and T. Kailath, "ESPRIT—a subspace rotation approach to estimation of parameters of cisoids in noise," *IEEE Trans. Acoustics, Speech, and Signal Processing*, vol. 34, pp. 1340–1342, Oct. 1986.

[10] H. Van hamme, "High resolution frequency-domain reflectometry by estimation of modulated superimposed complex sinusoids," in *Conf. Record of the IEEE Instrumentation and Measurement Technology Conference*, New York, May 12–14, 1992, pp. 106–113.

[11] J. S. Izadian and S. M. Izadian, *Microwave Transition Design.* Norwood, MA: Artech House, 1988, ch. 2.

[12] E. H. Fooks and R. A. Zakarevičius, *Microwave Engineering Using Microstrip Circuits.* New York: Prentice Hall, 1990, ch. 3.5.